



# **Development of a Predictive Oxidation Tool for the Annealing Process**

## **Modelling Oxidation Behaviour in Advanced High- Strength Steels (AHSS)**

*An AmbarPro Whitepaper on Custom Process Modelling and Simulation*

# Executive Summary

The increasing adoption of Advanced High-Strength Steels (AHSS) in the automotive industry is driven by the need to reduce vehicle mass and CO<sub>2</sub> emissions while maintaining structural performance and cost efficiency. However, the complex selective-oxidation phenomena occurring during annealing pose significant challenges for hot-dip galvanizing, as surface oxides of Mn and Si inhibit the formation of the Fe<sub>2</sub>Al<sub>5</sub> inhibition layer required for proper zinc adhesion. Industrial control of these reactions remains difficult, and existing models are often too simplified, computationally expensive, or impractical for routine use.

This work presents the development of a comprehensive, physics-based oxidation model that predicts internal oxidation, external selective oxidation, and FeO scale evolution under non-isothermal annealing conditions. The work presented here utilizes a proven physics-driven methodology, refined in industrial practice, and is presented as a representative example of AmbarPro's custom modelling capabilities for complex metallurgical challenges. The model couples multicomponent diffusion, thermodynamic oxide stability, precipitation kinetics, and moving-boundary behaviour within a unified 1-D numerical framework solved via an explicit finite-difference scheme. A dedicated precipitation algorithm ensures thermodynamic consistency under non-differentiable reaction conditions.

The model is implemented as a standalone custom simulation tool that reflects AmbarPro's modelling and simulation capabilities. With a modular architecture, integrated solver, and user-friendly graphical interface, it is validated against literature data and laboratory experiments. Despite its increased physical complexity, it achieves significantly reduced computation times (5–7 hours) relative to previous 12–24-hour models.

The resulting tool provides a practical and reliable platform for predicting selective oxidation under realistic furnace conditions, reducing reliance on trial-and-error process tuning and enabling more robust control of galvanizability in AHSS production.

## ***AmbarPro Modelling Approach***

AmbarPro's modelling approach is based on the development of custom, physics-driven simulation tools tailored to specific industrial processes rather than the use of overly generic or black-box software solutions. Each model is constructed by explicitly identifying the dominant physical mechanisms governing the process and integrating them into a unified numerical framework that balances physical fidelity, computational efficiency, and practical usability.

Key features of this approach include the tight coupling of transport phenomena, thermodynamics, and kinetics; the use of numerically robust yet transparent solution strategies; and a modular architecture that allows models to be extended or adapted as process requirements evolve. Equal emphasis is placed on computational performance and user accessibility, ensuring that advanced models can be deployed as practical engineering tools rather than remaining purely academic implementations.

## ***Key Findings***

- The developed model successfully captures the coupled nature of internal oxidation, external selective oxidation, and FeO scale growth during non-isothermal annealing of AHSS within a unified framework.
- Explicit treatment of multicomponent diffusion, thermodynamic oxide stability, and precipitation kinetics enables the model to reproduce experimentally observed oxidation trends reported in the literature, including the location of selective-oxide fronts and surface enrichment behaviour.
- The inclusion of FeO scale growth and reduction through a moving-boundary formulation allows realistic simulation of industrial furnace sequences, including transitions between oxidising and reducing atmospheres.
- Despite its increased physical complexity, the model achieves substantially reduced computation times (5–7 hours) compared to earlier-generation oxidation models, which typically required 12–24 hours under simplified assumptions.
- The modular numerical architecture and standalone graphical user interface enable the model to be used as a practical engineering tool, supporting rapid scenario analysis and reducing reliance on trial-and-error furnace adjustments.

## Introduction & Background

The automotive industry is undergoing a profound transformation driven by increasingly stringent global regulations on greenhouse gas emissions. To meet ambitious CO<sub>2</sub> reduction targets, vehicle manufacturers are under pressure to reduce vehicle mass while simultaneously improving safety performance and maintaining affordability. Advanced High-Strength Steels (AHSS) have emerged as a key enabler of this transition, offering a unique combination of high strength, formability, and cost-effectiveness that allows significant weight reduction without compromising structural integrity.

AHSS grades achieve yield strengths above 550 MPa and tensile strengths exceeding 700 MPa—levels unattainable with conventional steels—through carefully designed chemistries and multiphase microstructures [1]. As a result, replacing conventional steels with AHSS in the body-in-white can reduce vehicle mass by up to 17–25%, corresponding to several tons of CO<sub>2</sub> savings over a vehicle's lifetime. Life cycle assessments consistently show that AHSS delivers lower total emissions than alternative lightweight materials, while remaining economically viable for high-volume production. Additionally, AHSS is the only material to achieve reductions in all life cycle phases [2]. The widespread adoption of AHSS therefore represents one of the most effective and scalable strategies for reducing automotive emissions worldwide.

Despite these advantages, steel remains susceptible to corrosion and must be protected through continuous hot-dip galvanizing. Before the galvanizing step, the steel strip is exposed to an annealing treatment in order to reduce its internal stress and achieve the desired microstructure. Figure 1 shows the typical general furnace sections in the annealing process as well as an example of a temperature-time annealing cycle with intermediate oxidation.

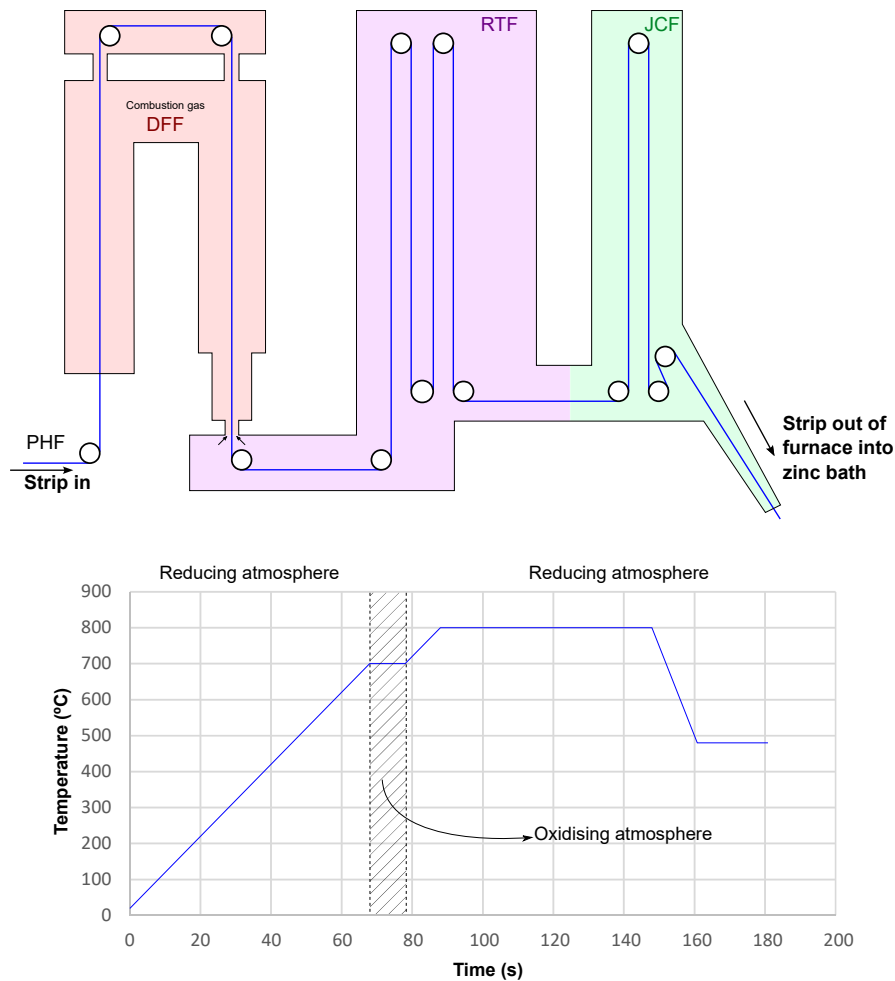


**Figure 1. Typical annealing treatment process (top) and typical temperature-time process conditions of the galvanizing process (bottom)**

During this thermal cycle, however, selective oxidation of alloying elements such as Mn and Si can occur at the steel surface, especially under the carefully balanced atmospheres of industrial annealing furnaces. These surface oxides inhibit the formation of the  $Fe_2Al_5$  inhibition layer required for proper zinc adhesion, leading to coating defects including bare spots, dewetting, and delamination. Such defects have significant economic consequences and pose major process-control challenges for steel producers.

Selective oxidation is influenced by numerous interacting factors: steel composition, diffusion kinetics, local oxygen partial pressure, dew point, temperature profiles, and furnace-zone residence times. Industrially, the process window is narrow, as the annealing parameters must simultaneously satisfy microstructural requirements and ensure galvanizability. Traditionally, determining appropriate furnace settings has relied heavily on trial and error, consuming time, materials, and production capacity.

This complexity underscores the need for accurate, physics-based modelling tools that can predict surface oxidation behaviour under realistic processing conditions. Such models must couple multicomponent diffusion, thermodynamic oxide stability, internal and external oxidation phenomena, and the dynamic reduction and growth of the FeO scale across non-isothermal furnace zones. Historically, these models have been computationally demanding and difficult to integrate into production workflows, limiting their practical use.

To address these challenges, the present work demonstrates the development of a predictive oxidation model—presented here as an example of AmbarPro’s custom simulation capabilities—capable of capturing the key mechanisms governing selective oxidation during the annealing of AHSS. This project illustrates how AmbarPro enables the construction of complex, multi-physics models that are computationally efficient, user-friendly, and adaptable to industrial needs. The oxidation model serves as a representative example of AmbarPro’s capabilities in delivering advanced modelling solutions tailored to real-world metallurgical problems.

## Problem Statement & Technical Challenges

The annealing of AHSS is a critical step in automotive steel processing, governing both the mechanical properties of the final product and its suitability for subsequent hot-dip galvanizing. However, controlling surface oxidation during annealing remains one of the most complex and persistent challenges for steel manufacturers.

Typically, AHSS contain mainly iron (>97 %wt), carbon, and manganese as the major alloying elements, and some other minor alloying elements, such as Si, Cr, V, Al, B and Ti. These alloying elements in contact with an oxidising agent produce selective oxides. Selective oxidation will occur when there are one or more oxides that are stable and the oxidising conditions are not enough to oxidise the major element: iron. That implies that the selective alloying elements form selective oxides even with the reducing atmosphere conditions of the reduction step in the furnace, i.e., the radiant tubes furnace (RTF). As seen in Figure 2, in a normal direct fired furnace (DFF) operation the atmosphere is composed of waste combustion gases with no free oxygen and a dew point higher than +60 °C; here, a relatively thin iron oxide layer (<100 nm) is formed. When the steel is introduced in the RTF section, the scale layer is reduced in a short period of time, and the selective alloying elements, which are diffusing towards the surface, have sufficient time to reach it and react with the oxidising agents in the atmosphere, forming subsequently selective oxides at the surface (external oxides).

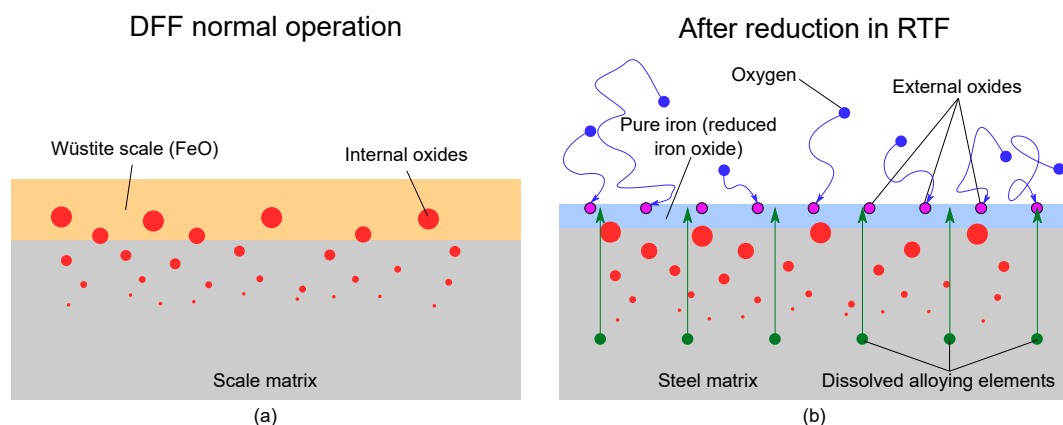


**Figure 2. Schematic representation of the oxide concentration in the steel surface region in a normal operation after (a) oxidation in the direct fired furnace (DFF) and after (b) reduction in the radiant tubes furnace (RTF)**

If there is a considerable concentration of selective oxides on the surface of the steel sheet, the zinc is not properly adhered and that may cause some superficial defects, such as dewetting, bare spots and/or delamination during bending. These superficial defects decrease the quality of the steel, or render it unusable, producing subsequently an economic loss.

One of the most practical solutions to avoid the presence of selective oxides on the sheet surface is to pre-oxidise the surface either by increasing the air/fuel-gas ratio in the DFF or injecting oxygen in a zone of the furnace so that a thicker oxide layer is formed. With the presence of a thicker iron oxide layer, the time necessary to reduce completely the wüstite layer in the reducing atmosphere (RTF) is increased, leaving less time to the selective alloying elements to diffuse towards the surface and reach it. Furthermore, the distance that the selective elements have to travel to reach the surface once the wüstite layer has been entirely reduced is increased. Figure 3 shows a schematic representation of what happens in the steel when pre-oxidation is used. However, the FeO scale cannot be extremely thick due to the risk of not being able to reduce it completely in the reduction step, leading to delamination of the Zn layer together with the freshly reduced iron layer (substrate delamination).

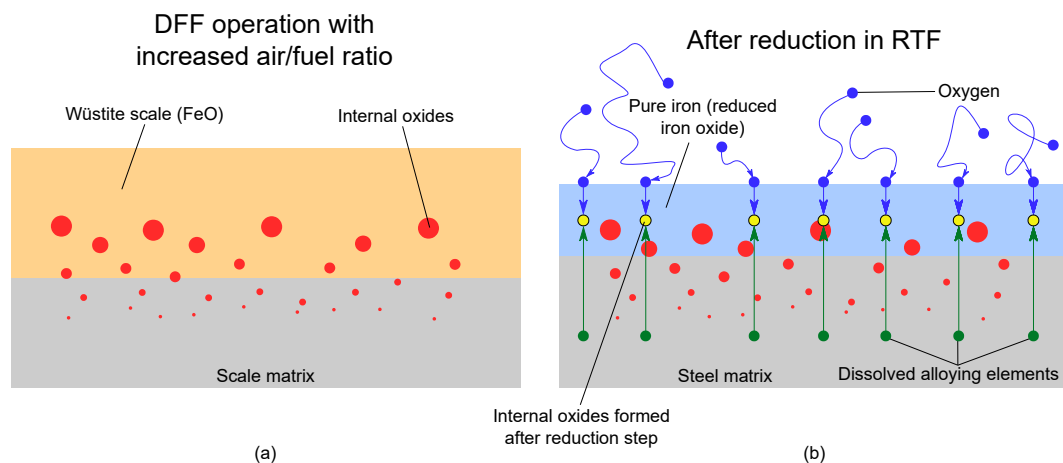


**Figure 3. Schematic representation of the oxides concentration in the steel surface region in an operation including an oxygen bar after (a) oxidation with the oxygen bar and after (b) reduction in the RTF**

Accurate prediction of whether selective oxidation will occur under a given set of processing conditions is therefore essential. Yet, the oxidation behaviour of AHSS during annealing depends on a highly coupled set of physical and chemical phenomena:

- Multicomponent diffusion of Mn, Si, C, and O within the steel.
- Thermodynamic competition between internal oxidation, external selective oxidation, and FeO scale formation.
- Dynamic reduction and re-oxidation across furnace zones (DFF, RTF, JCF), each with distinct temperatures, dew points, and gas chemistries.
- Moving boundary conditions, as the FeO scale grows and shrinks during the annealing cycle.
- Strong temperature dependence of diffusivities, solubilities, and reaction rates in a non-isothermal environment.

Industrial process control adds an additional layer of complexity. Furnace parameters such as temperature profile and strip speed are dictated primarily by microstructural targets, leaving only limited flexibility in atmosphere adjustments. This creates a narrow operating window in which both microstructure and surface quality must be simultaneously satisfied. Historically, manufacturers have relied on trial-and-error adjustments to furnace atmospheres—an approach that consumes significant time, energy, and material without guaranteeing optimal results.

Existing oxidation models offer partial solutions, but they often suffer from one or more limitations:

- Internal and external oxidation are treated independently, despite their interacting nature.
- FeO scale dynamics are oversimplified, neglecting moving boundaries and time-dependent transitions.
- Computational times are prohibitive, with some legacy models requiring 12–24 hours for a single simulation.
- Tools require specialized software knowledge, limiting adoption by process engineers and production teams.

As a result, the industry still lacks a practical, physics-based tool capable of reliably predicting oxidation behaviour under realistic production conditions.

The objective of this project is to address these shortcomings by developing a custom, 1-D, non-isothermal oxidation model that integrates diffusion, thermodynamics, precipitation kinetics, and FeO scale growth into a unified framework. The model must:

- Predict whether selective oxides form at the steel surface.
- Quantify the amount and type of surface oxides when external oxidation occurs.
- Capture transitions between internal and external oxidation regimes.
- Handle dynamic FeO scale growth using moving boundaries.
- Remain computationally efficient for practical use (target runtime on simplified cases: 1–3 hours).
- Operate as a standalone, offline tool without thermodynamic database dependencies.
- Provide a user-friendly interface enabling non-specialists to run simulations and export results.

This combination of requirements makes selective oxidation modelling an ideal demonstration of AmbarPro's capabilities—showcasing its strengths in handling multi-physics simulations, dynamic boundaries, numerical optimization, and user-oriented tool development.

## Modelling and Computational Implementation

### Mathematical Model and Numerical Methods

The selective oxidation behaviour of AHSS during annealing arises from tightly coupled physicochemical mechanisms involving diffusion, thermodynamics, phase transformations (precipitation), and evolution of moving boundaries. Modelling these interactions requires a numerical framework capable of resolving steep concentration gradients, strongly temperature-dependent properties, and the continuous competition between internal oxidation, external selective oxidation, and FeO scale growth. Additionally, the precipitation mechanism introduces non-differentiable behaviour, further increasing the complexity of the problem.

The governing equations consist of partial differential equations (PDEs) describing the transient mass balance of each species. Concentration profiles evolve according to extended Fick's second law including reaction kinetics, with diffusion coefficients expressed as a function of temperature. Both the initial conditions and the boundary conditions of the system are dependent on the initial alloy concentrations and on the instantaneous FeO scale thickness. The following representative PDE is shown to illustrate the mathematical complexity of the underlying model and the nonlinear couplings present in the system:

$$\frac{\partial C_i(x, t)}{\partial t} = D_i(T) \frac{\partial^2 C_i(x, t)}{\partial x^2} - \sum_j v_{i,j} \frac{\partial C_j(x, t)}{\partial t}$$

where  $C_i(x, t)$  denotes the concentration of species  $i$ , with  $i \in \{\text{Si, Mn, or O}\}$  and  $C_j(x, t)$  is the concentration of oxide  $j$ , with  $j \in \{\text{SiO}_2, \text{MnO, or Mn}_2\text{SiO}_4\}$ , each defined as a function of position  $x$  and time  $t$ ,  $v_{i,j}$  denotes the stoichiometric coefficient of alloying element  $i$  in oxide  $j$ , and  $D_i(T)$  denotes the temperature-dependent diffusion coefficient of species  $i$ .

The system is numerically implemented and solved by applying an explicit finite-difference method proposed by Crank [3]. The domain of the problem (e.g., time and space) is divided into a grid of points:

- $x, x+1, \dots, x+N$  in space, with uniform spacing  $\Delta x$  and
- $t, t+1, \dots, t+N$  in time, with uniform time step  $\Delta t$ .

The spatial and temporal derivatives in the system of PDE's are replaced by finite-difference approximations. Applying this discretization to the illustrative PDE yields:

$$C_{i,x}^{t+1} = C_{i,x}^t + \frac{D_i \Delta t}{\Delta x^2} (C_{i,x-1}^t - 2C_{i,x}^t + C_{i,x+1}^t) - \sum_j v_{i,j} (C_{j,x}^{t+1} - C_{j,x}^t)$$

The precipitation of the different oxides adds an additional layer of complexity: although the process is continuous, it is not differentiable. In practice, the thermodynamics allow only two possible outcomes:

- If the stoichiometric product of the relevant alloying-element concentrations is lower than the solubility product, the selective oxide does not precipitate.
- If the stoichiometric product equals the solubility product, the selective oxide becomes thermodynamically stable, and its precipitated amount is positive.

Figure 4 shows the thermodynamic regions where selective oxides can precipitate as a function of the concentration of Si and Mn at each point of the steel sheet. Within the region defined by the dash-dot lines, no selective oxides precipitate. As the oxygen concentration decreases, this region widens; conversely, it shrinks when oxygen concentration increases. When any of the reactant concentrations (Si, Mn or O) exceed the threshold, precipitation occurs immediately due to the fast reaction kinetics.

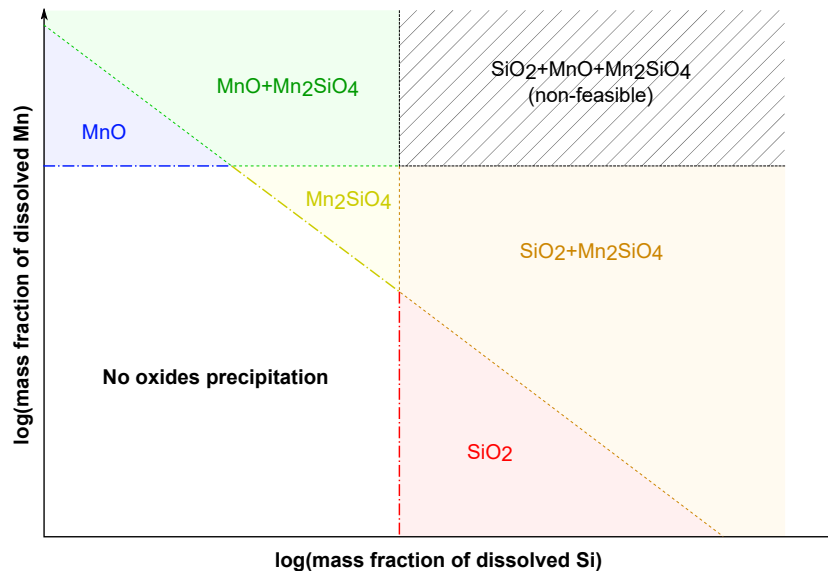


Figure 4. Thermodynamic boundaries of a Fe-Si-Mn system with formation of simple and mixed oxides for a fixed oxygen concentration

Because discretization increases the local concentrations from time  $t$  to time  $t + \Delta t$ , the solution may cross into a region where precipitation is thermodynamically required. However, determining which oxide (or combination of oxides) precipitates is not straightforward. To address this, a dedicated precipitation algorithm was developed to ensure consistency with thermodynamics and to prevent physically incorrect precipitation pathways. The simplified algorithm is illustrated in Figure 5.

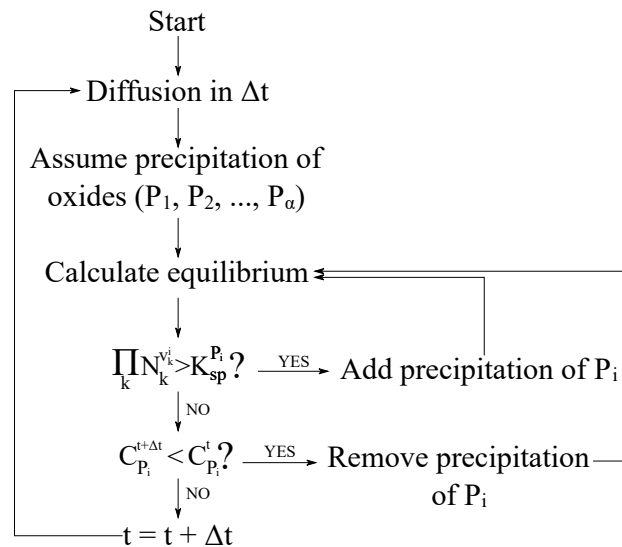


Figure 5. Precipitation algorithm when no re-dissolution is allowed

Furthermore, the formation of an FeO scale layer adds complexity by introducing a moving-boundary problem: the FeO–gas and the FeO–steel interfaces shift as the FeO scale grows or is reduced. Consequently, the computational grid must adapt over time by shifting inward or adjusting its resolution as the scale thickness evolves.

## Computational Algorithm and Graphical User Interface

The model was implemented as a custom numerical tool capable of simulating the coupled diffusion, precipitation, and scale-growth mechanisms within a unified 1-D domain that represents the surface-near region of an AHSS sheet undergoing a full non-isothermal annealing cycle. The complete algorithm, including all PDEs, precipitation logic, and moving boundary treatment, was implemented in MATLAB.

This project showcases AmbarPro's strengths in building advanced, tailor-made simulation tools:

- **Custom Solver Integration:** The entire numerical algorithm, including PDE solvers and dynamic precipitation routines, was integrated as a custom modelling tool.
- **Modular Architecture:** The physics, thermodynamics, and boundary-condition modules were structured for extensibility, enabling additional alloying elements or selective oxides to be incorporated.
- **Graphical User Interface:** A dedicated GUI enables users to define temperature profiles, steel compositions, furnace atmospheres, and numerical parameters without interacting with the underlying code.
- **Data Export:** Simulation outputs—including oxide-depth profiles, FeO scale evolution, and surface enrichment data—are automatically compiled into Excel-compatible files for analysis.
- **Reduced Execution Time:** The optimized implementation significantly outperforms traditional MATLAB models, demonstrating AmbarPro's ability to accelerate computational workflows.

The model inputs and outputs are shown in Table 1.

Table 1. Oxidation tool inputs and outputs

Inputs	Outputs (.xlsx file)
<ul style="list-style-type: none"><li>• Steel composition</li><li>• Temperature-time profile of the annealing cycle</li><li>• Atmosphere conditions at each furnace section</li><li>• FeO scale-growth kinetic parameters</li><li>• Spatial discretization settings</li></ul>	<ul style="list-style-type: none"><li>• Simulation conditions and parameters</li><li>• Dissolved O, Mn and Si at each depth</li><li>• MnO, SiO<sub>2</sub> and Mn<sub>2</sub>SiO<sub>4</sub> concentration profiles</li><li>• Simulation metadata</li></ul>

In addition to the numerical implementation in MATLAB, a graphical user interface (GUI) was developed so that people without modelling experience can intuitively set up simulations and evaluate new annealing cycles for AHSS (see Figure 6).

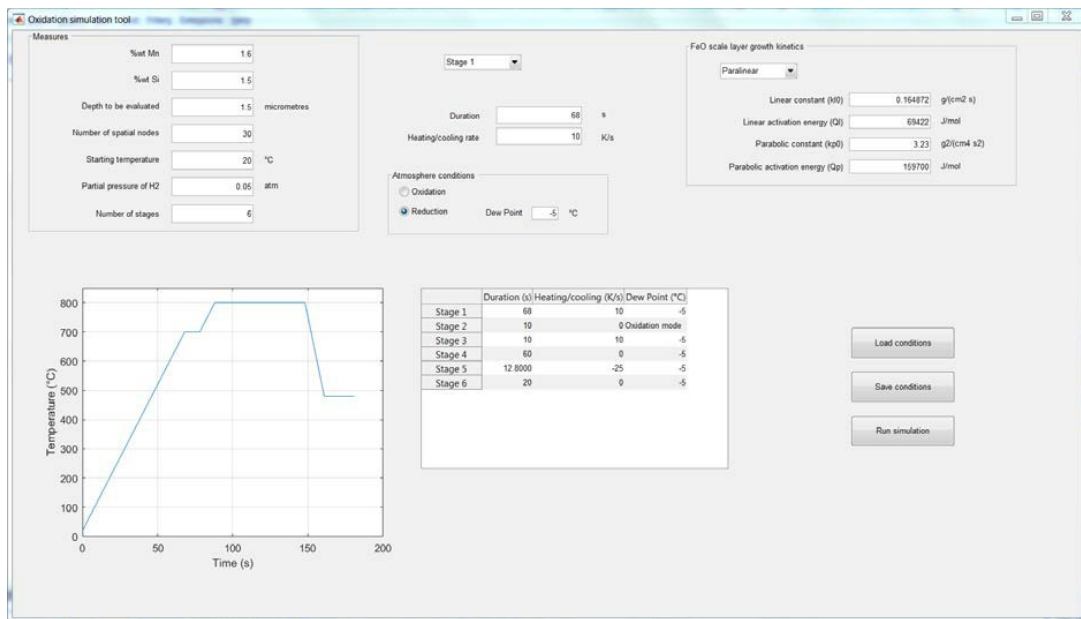


Figure 6. Main GUI window of the Predictive Oxidation Tool

## Results

The numerical implementation and the physical predictions of the model were validated using published experimental and simulation data. Two levels of validation were carried out:

1. numerical validation, ensuring that the discretisation and solver behave as expected, and
2. physical validation, comparing model predictions with qualitative and semi-quantitative oxidation behaviour described in the literature.

## Numerical Validation

The numerical scheme was benchmarked against the work of Huin et al. [4]. A simulation was performed for a steel containing 1.235 %wt Mn and 0.12 %wt Si, under a dew point of +15°C. Figure 7 compares the concentration profiles of total Mn and Si obtained with the oxidation tool to those published by Huin et al. The agreement is strong: the predicted trends and magnitudes match closely, with only minor deviations. These small differences are attributed to discretisation-resolution effects in the original paper, rather than discrepancies in the implemented physics.

It should be noted that this validation case corresponds to a thermal treatment without oxidation, and therefore without FeO scale formation, which isolates diffusion and precipitation effects for clearer comparison.

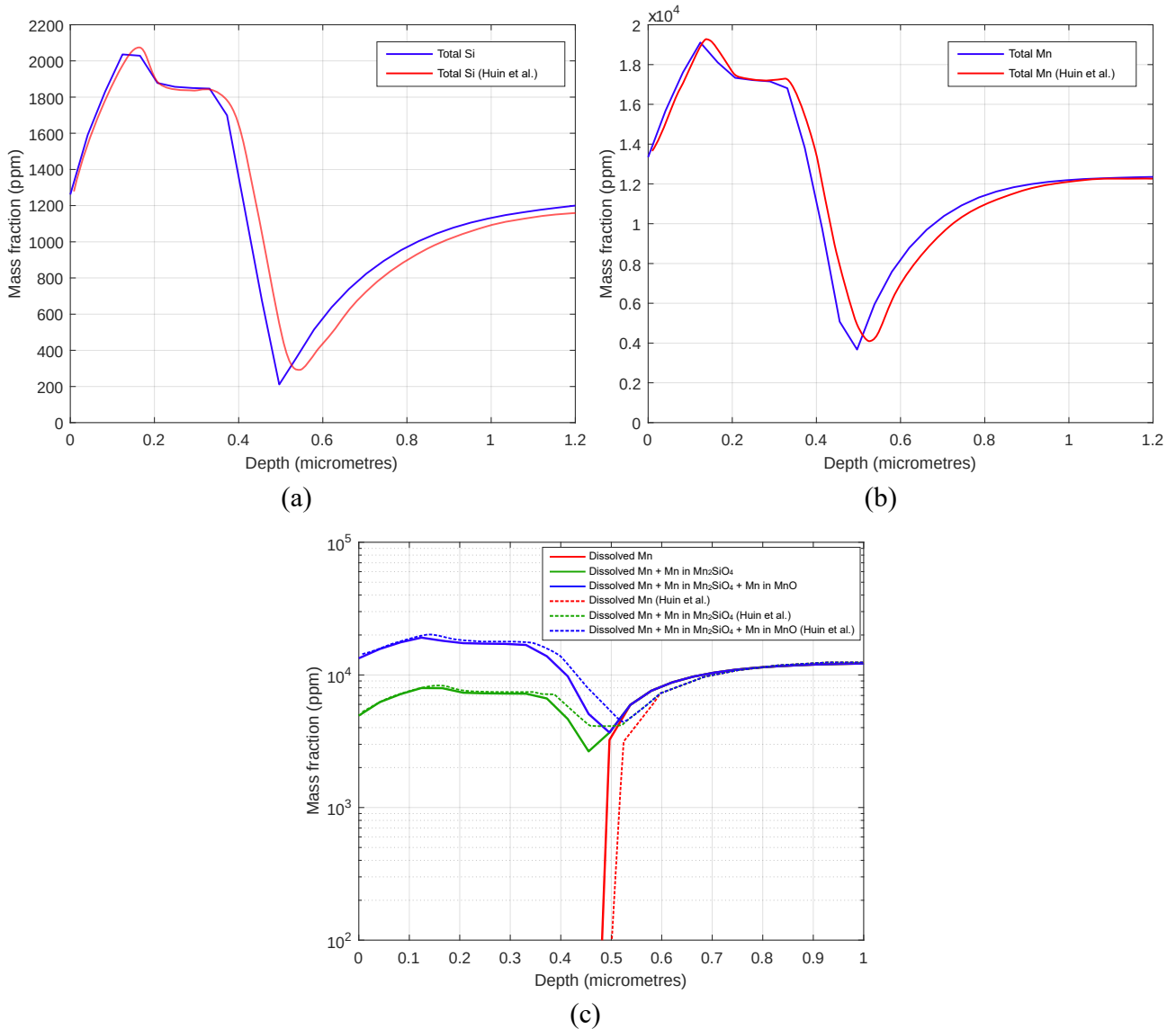


**Figure 7. Comparison of concentration profiles of (a) total Si, (b) total Mn, and (c) Mn in different forms for a Fe-Si-Mn alloy at DP=-15°C after a non-isothermal treatment, considering only the precipitation of simple and mixed oxides, and compared with the results of Huin et al. [4]**

## Qualitative Validation Under Reducing Conditions

Because this work represents the first non-isothermal selective-oxidation model that explicitly includes FeO scale formation and reduction, a full quantitative validation of the complete model is not yet feasible due to the scarcity of published datasets. However, a qualitative comparison was performed using results from isothermal annealing experiments under reducing conditions [5]. A laboratory sample was analysed via SEM after short exposure to a reducing atmosphere. The same conditions were simulated with the oxidation tool.

As shown in Figure 8, the SEM image reveals a diffuse front of selective oxides located roughly around 1.1  $\mu\text{m}$ . The model predicts a rapid decrease in total oxide concentration beginning at 1.2  $\mu\text{m}$  and extending to approximately 1.65  $\mu\text{m}$ . Given the limited resolution of the SEM image and inherent uncertainty in manually identifying the oxide front, the results are considered consistent. A more quantitative experimental measurement would further strengthen this validation.

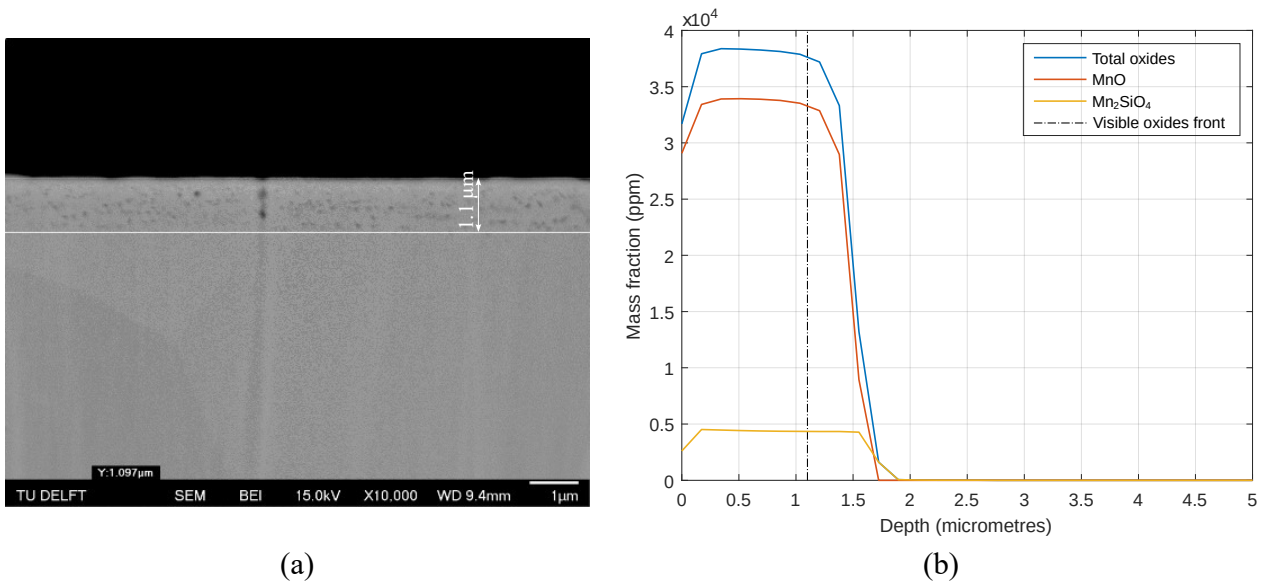


Figure 8. (a) SEM image of a lab sample after an isothermal annealing treatment [5] and (b) simulation results using the oxidation tool

## Validation Including FeO Scale Formation

Quantitative validation of FeO scale growth remains challenging due to the limited amount of published data combining dew point, time-temperature paths, and oxide characterisation. Nevertheless, an indirect validation was enabled using adhesion test results from Norden et al. [6]

Norden et al. investigated two non-isothermal annealing cycles for a steel containing 1.6 wt% Mn, 1.5 wt% Si, 0.16 wt% C and <0.05 wt% Al, at several dew points. One of the treatments included an isothermal pre-oxidation step at 700 °C. Each cycle was simulated using the oxidation tool with parabolic FeO scale-growth kinetics.

The authors reported adhesion outcomes (good/poor) using the standard ball impact test (BIT). They showed that poor adhesion correlates strongly with the presence of SiO<sub>2</sub> at the surface, as it suppresses Fe<sub>2</sub>Al<sub>5</sub> inhibition-layer formation more drastically than MnO or Mn<sub>2</sub>SiO<sub>4</sub>. Table 2 summarises the experimental BIT results and the predicted surface SiO<sub>2</sub> concentration obtained using the oxidation tool.

Table 2. Adhesion results obtained by Norden et al. [6] and predicted SiO<sub>2</sub> concentration at the surface by the oxidation tool

DP (°C)	Pre-oxidation	Adhesion result (from Norden et al. [6])	Predicted SiO <sub>2</sub> superficial concentration (%wt)
-5	No	Good	10.2
-25	No	Poor	17.0
-5	Yes	Good	1.1
-25	Yes	Good	11.0
-40	Yes	Poor	12.8

The results clearly demonstrate a correlation between surface  $\text{SiO}_2$  and adhesion quality. The model predicts a transition zone between good and poor adhesion:

- Good adhesion for  $\text{SiO}_2 < 11 \text{ wt}\%$
- Poor adhesion for  $\text{SiO}_2 > 12.8 \text{ wt}\%$

These thresholds are fully consistent with the trends observed experimentally by Norden et al. [6].

## Execution Time and Performance

Although the new model incorporates significantly more physical complexity than previous internal tools, including the following:

- multiple alloying species,
- simultaneous internal and external oxidation
- non-differentiable precipitation behaviour,
- evolution of a moving FeO boundary, and
- full non-isothermal furnace cycles,

the new implementation achieves substantially shorter computation times. Earlier generation oxidation models, developed in comparable industrial contexts, typically required 12–24 hours to complete a simulation, even with simplified assumptions.

The new implementation reduces the runtime to 5–7 hours, while modelling a much more comprehensive set of coupled mechanisms. This improvement highlights the efficiency of the numerical strategy and the value of integrating the solver within the AmbarPro toolchain, enabling faster iteration and broader industrial applicability.

## Conclusion

This work demonstrates the successful development of a comprehensive, physics-based oxidation model capable of predicting selective-oxidation behaviour during the annealing of Advanced High-Strength Steels (AHSS). By integrating multicomponent diffusion, thermodynamic stability, precipitation kinetics, and FeO scale growth into a unified 1-D, non-isothermal framework, the model captures the key mechanisms that govern surface chemistry under industrial galvanizing conditions. The explicit finite-difference formulation, combined with a dedicated precipitation routine and a moving-boundary treatment for the FeO scale, enables accurate numerical representation of a highly coupled and non-linear system.

Validation activities confirm both the numerical consistency of the implementation and its ability to reproduce experimentally observed oxidation trends. The model accurately predicts diffusion-controlled segregation during non-oxidizing cycles, reproduces the location of the selective-oxide front under reducing conditions, and correctly identifies the relationship between surface  $\text{SiO}_2$  enrichment and coating adhesion reported in independent studies. These results provide strong evidence that the tool captures the dominant physical mechanisms governing selective oxidation in AHSS.

A major outcome of this project is the significant improvement in computational efficiency. Despite incorporating far greater physical complexity than previous internal models—including simultaneous internal and external oxidation, non-differentiable precipitation behaviour, and dynamic FeO boundary evolution—the new implementation completes full non-isothermal simulations in 5–7 hours, compared to the 12–24 hours required by earlier tools with more restrictive assumptions. This reduction in runtime substantially enhances the model's practicality for industrial and research workflows.

Its presentation within the AmbarPro framework illustrates how such models can be transformed into robust, user-oriented industrial tools. Its modular numerical architecture, integrated solver, and dedicated graphical user interface make the tool accessible to non-specialist users, allow rapid scenario definition, and enable straightforward comparison of annealing strategies. Automated data export facilitates downstream analysis and supports integration into process-development pipelines. Together, these features highlight AmbarPro's capabilities in delivering robust, configurable, and computationally efficient multi-physics simulations tailored to complex metallurgical challenges.

Overall, the predictive oxidation tool represents a significant step toward reducing reliance on trial-and-error furnace adjustments, improving galvanizability control, and supporting the broader industrial adoption of AHSS. While future work should focus on extending the model to additional alloying elements, refining thermodynamic parameters, and incorporating more detailed FeO scale kinetics, the current version provides a validated and operationally practical foundation for process optimisation. The project illustrates how advanced modelling methodologies—combined with AmbarPro's simulation framework—can accelerate innovation and provide meaningful support to modern steelmaking operations.

## References

- [1] V. Aghaei Lashgari, Internal and external oxidation of manganese in advanced high strength steels, s.n., S.I., 2014.
- [2] World Steel Association, Sustainable steel: At the core of a green economy, Rue Colonel Bourg 120 (2012).
- [3] J. Crank, The mathematics of diffusion, 2. ed., repr, Univ. Pr, Oxford, 2011.
- [4] D. Huin, P. Flauder, J.-B. Leblond, Numerical Simulation of Internal Oxidation of Steels during Annealing Treatments, *Oxid Met* 64 (2005) 131–167. <https://doi.org/10.1007/s11085-005-5718-x>.
- [5] W. Mao, Oxidation Phenomena in Advanced High Strength Steels: Modelling and Experiment, Delft University of Technology, 2018. <https://doi.org/10.4233/UUID:3E978189-4FD7-4358-840E-B995416BEDEF>.
- [6] M. Norden, M. Blumenau, R. Schönenberg, Recent Trends in Hot-Dip Galvanizing of Advanced High-Strength Steel at ThyssenKrupp Steel Europe, in: 2012: pp. 67–73.